Adaptation and Optimization of Biological Transport Networks

Dan Hu[1,*] and David Cai[1,2,3,†]

[1]*Department of Mathematics, Institute of Natural Sciences, and MOE-LSC, Shanghai Jiao Tong University, Shanghai 200240, China*
[2]*Courant Institute and Center for Neural Science, New York University, New York, New York 10012, USA*
[3]*NYUAD Institute, New York University Abu Dhabi, PO Box 129188 Abu Dhabi, United Arab Emirates*

(Received 8 March 2013; published 25 September 2013)

It has been hypothesized that topological structures of biological transport networks are consequences of energy optimization. Motivated by experimental observation, we propose that adaptation dynamics may underlie this optimization. In contrast to the global nature of optimization, our adaptation dynamics responds only to local information and can naturally incorporate fluctuations in flow distributions. The adaptation dynamics minimizes the global energy consumption to produce optimal networks, which may possess hierarchical loop structures in the presence of strong fluctuations in flow distribution. We further show that there may exist a new phase transition as there is a critical open probability of sinks, above which there are only trees for network structures whereas below which loops begin to emerge.

DOI: 10.1103/PhysRevLett.111.138701 PACS numbers: 89.75.Hc, 89.75.Da, 89.75.Fb, 89.75.Kd

There has long been scientific interest in biological transport networks, which are ubiquitous in living systems. Blood vasculature and leaf venation are examples of such networks. These networks may exhibit tree or loop structures, and afford great benefit to biological systems [1–4]; e.g., the elastic property of a leaf is intimately related to the structure of its leaf venation [2]. These networks have been studied in the optimization framework, where the energy consumption within the networks is minimized under the constraint of constant total material cost [3–7]. Assuming that the material cost for an edge of the network is proportional to a power law C^γ, where C is the conductance of the edge, the work of Refs. [3–7] has shown that the optimal networks exhibit a phase transition at $\gamma = 1$, with a uniform sheet [3,5,8] for $\gamma > 1$ and a loopless tree for $\gamma < 1$. However, there are, in general, many loops in biological transport networks [1–4,9]. Animals and plants may benefit from loop structures in many ways. For example, loops are important in mitigating damages of networks [3] and optimizing energy consumption with fluctuating flow distributions [3,4].

Natural selection may give rise to optimal networks [1–7,9]. However, optimization principles often are global in nature and are silent about the mechanistic processes for living systems to adapt to such optimal structures. For blood circulation systems, it has been observed in experiment that blood vessels can sense the wall shear stress [10] and adapt their diameters according to the stress [11–14]. An adaptation process is described mathematically as a dynamical system in response to changes of local wall shear stress [11–14]. The previous modeling work showed that the optimal vessel radius of a blood vessel tree can be achieved through adaptation [15]. It has been found [13] that the adaptation to wall shear stress can lead to topological changes of the vessel network structure, and this adaptation is related to the optimization of energy consumption of the network. An adaptive model is also introduced in the study of the networks formed by slime mold *Physarum polycephalum* [16], where networks at the steady states of adaptation are compared with networks with optimal total edge length.

In this Letter, we propose an adaptation dynamics in response to local information for biological transport networks and study its relation to optimization principles. First, we introduce a total energy consumption function for a general class of biological transport networks. This function is similar to those in Refs. [3–6]; however, it includes material cost as part of the energy consumption. Second, we construct an adaptation dynamics based on experimental results. Third, in adaptation dynamics, we incorporate flow fluctuations due to changes of the state of flow sinks (sources), which are generally observed in biological transport networks. For example, in leaf venation, fluctuations arise from the open-close switch of stomata [3]; in circulation systems, it is a result of the flow regulation of capillary flows, which also exhibit fluctuating behavior [14]; flow fluctuations are also observed in the network of a *Physarum polycephalum* [16]. We model these general fluctuations by fluctuating flow sinks (sources) at nodes of transport network and show that they can be captured by a model with open probability p for sinks (sources) in the network. In contrast to the general global nature of optimization principle, we emphasize that, in our model, the driving force of the adaptation depends only on local information. For both cases of fixed- and fluctuating-flow distribution, we show that the adaptation dynamics in response to local information leads to a continuous decrease of the total energy consumption and reaches an optimal network at the steady state.

What kind of configurations of optimal networks can be achieved through adaptation is one of the central issues of biological transport networks. As noted above, loops appear generally in biological transport networks under fluctuating flow distributions. Our results show that loopy networks can be stable under the adaptation and this may give rise to the adaptation stability of loopy biological structures, such as loops formed by arterial anastomosis. For the network of the open-close switch type of sinks with an open probability p, our numerical results indicate that there may be a new phase transition at a critical value p_c of the open probability. Above p_c, optimal networks are loopless, whereas below p_c the loop density increases as p decreases. Our results may provide new insight into how fluctuations in flow distributions may impact optimal structures of transport networks through this new phase transition.

Flow distribution.—Tubes form the edges of many biological transport networks, and flows in the tubes are the transport carrier. The Reynolds number in such a tube (except, e.g., in large blood vessels [12]) is usually very low and the flow is driven by the pressure drop on the two ends of the tube, $Q = C\Delta P$, where Q is the flow rate, C is the conductance, and ΔP is the pressure drop. The conductance C is usually determined by the geometry of the edge. For example, for a small blood vessel, which geometrically can be regarded as a cylinder, the blood flow in it can be well approximated by the Poiseuille flow. This yields the vessel conductance $C = (\pi D^4/128\eta L)$, where η is the viscosity of the blood, D and L are the diameter and length of the vessel, respectively. A leaf vein is usually a bundle of small tubes with similar diameters; thus, for the vein, $C = nC_0 = (\pi D_0^2 D^2/128\eta L)$, where n is the number of small tubes, C_0 and D_0 are the conductance and diameter of a single tube, respectively. For a leaf venation, there are flow sinks due to the evaporation process of leaves [3]. For blood vasculature, the metabolic flow regulation processes are capable of maintaining a relative steady mean flow rate in capillaries [14,17]. This provides the sinks for the arterial network and the sources for the venous network. Once the conductance for all segments and the flow sources and sinks are known, by analogy to an electric circuit one can calculate the flow distribution using Kirchoff's law, $\sum_k (P_k - P_j)C_i = s_j$, where P is the pressure, k and j are the indices of the two end nodes of edge i, C_i is the conductance of edge i, and s_j is the given strength of flow sink (or source) at node j. For nodes not connected by an edge, the conductance between them is set to 0.

Energy consumption and adaptation.—In this work, we are interested in the question of whether there is a common mechanism, i.e., adaptation dynamics, in response to local information that can evolve a biological transport network to its optimal structure. Importantly, we require that the driving force in adaptation be local, because communications can often be expensive. The energy consumption function includes two parts,

$$E = \sum_i \left(\frac{Q_i^2}{\tilde{C}_i} + c_0 \tilde{C}_i^{\gamma} \right) L_i,$$

where c_0 is a metabolic coefficient, the power γ is an intrinsic constant of the network, i is the index of an edge, and Q_i, L_i, and $\tilde{C}_i = C_i L_i$ are the flow, the length, and the *conductivity* of vessel i, respectively. The first part of the energy consumption is the power that incurs in flow delivery through the network. The second part is the material and metabolic cost contained in the network and the carrier such as blood cells. In Murray's theory [18], the metabolic cost for a blood vessel is proportional to the number of blood cells in it, which is proportional to its volume. Note that the volume is proportional to $\tilde{C}^{1/2}$ in this case; therefore, $\gamma = 1/2$ for blood vessel systems. For leaf venations, the material cost may also be proportional to the number of small tubes, which is proportional to $\tilde{C}_i$, and the metabolic cost may be due to the effective loss of the photosynthetic power at the area of the venation cells, which is proportional to $\tilde{C}_i^{1/2}$. From this point of view, the effective value of γ for leaf venation may be between 1/2 and 1. We note that the material cost is not regarded as a constraint in our approach but as part of the energy consumption, and the metabolic coefficient c_0 is not a Lagrangian multiplier but a measurable constant.

As discussed above, blood vessels can adapt their diameters in response to local wall shear stress [12–14]. Adaptive responses are also observed in other biological transport networks, such as *Physarum polycephalum* [16]. In previous works [12–14], a diameter-adaptation model of vessels $(dD/dt) = c'(\tau_w - \tau_e)D$ is used to explain experimental results, where τ_w and τ_e are the real and constant optimal wall shear stress, respectively. With the requirement that the dynamics be equivalent to the diameter-adaptation model for blood vessels in the sense of linearization and satisfies that $(dE/dt) \leq 0$, we propose an adaptation model for general biological transport networks

$$\frac{d\tilde{C}_i}{dt} = c\left(\frac{Q_i^2}{\tilde{C}_i^{\gamma+1}} - \tilde{\tau}_e^2 \right) \tilde{C}_i, \tag{1}$$

where the term $Q_i^2/\tilde{C}_i^{\gamma+1}$ is the driving stimulus of flow and $\tilde{\tau}_e^2 = \gamma c_0$ is the intrinsic decreasing stimulus. In particular, in the case of blood vessels, the driving stimulus is the square of wall shear stress, $Q_i^2/\tilde{C}_i^{\gamma+1} = \tau_{w,i}^2$, and $\tilde{\tau}_e$ is the optimal wall shear stress. As will be seen below, the quadratic form of the adaptation model (1) can be naturally generalized to include fluctuations in flow distributions. Because $(dE/dt) < 0$, the network reached at the steady state has a minimal energy consumption and possesses an optimal structure. One can also model adaptation dynamics with a constraint of constant material and metabolic cost, then it involves the nonlocal information of Lagrangian multipliers.

Flow fluctuations.—As can be seen from Kirchoff's law, once the conductances of all edges are known, the flow in an edge is determined by the state of sinks. As discussed above, flow fluctuations at sinks (sources) appear generally in biological transport networks. In the optimization model [3], a fixed source and a single moving sink, i.e., a single randomly chosen sink at any particular time, is introduced for each state, and the optimization [3] involves the average effect of all different single-moving-sink states. Conceptually, this study provides a possible explanation for the existence of loops in transport networks. In the optimization model [4], uncorrelated random *amplitudes* of sinks are introduced. For a given distribution of random sinks, it numerically examined the relation between γ and the loop density d_l, which is defined as the averaged ratio of the total number of loops in optimal networks to the maximal possible number of loops. In our work, we first assume that sinks are described by a general random variable. Later we will show that this general class of model can be captured by a model with open probability only. Note that the time scale of fluctuations in flow distributions in biological transport networks is typically much smaller than that of adaptation [3,14]. Therefore, we can average the adaptation stimulus over all different configurations as the effective adaptation stimulus and obtain a deterministic dynamics

$$\frac{d\tilde{C}_i}{dt} = c'\left(\frac{\langle Q_i^2\rangle}{\tilde{C}_i^{\gamma+1}} - \tilde{\tau}_e^2\right)\tilde{C}_i, \tag{2}$$

where $\langle\cdot\rangle$ denotes averaging over all the configurations with all possible combinations of states of sources and sinks. In this case, the average energy consumption function becomes $\bar{E} = \sum_i((\langle Q_i^2\rangle/\tilde{C}_i) + c_2\tilde{C}_i^{\gamma})L_i$. We can again show that, under the adaptation dynamics (2), $\bar{E}$ decreases continuously and reaches optimal networks at the steady state.

Clearly, Monte Carlo methods can be used in simulation to take into account fluctuations. However, we will derive an exact expression below for the averaged stimulus which is useful in understanding the behavior of the system and in designing fast numerical methods. Without loss of generality, we consider N-node networks with only one source node and $N-1$ sink nodes. In this case, the states of all the sinks determine the flow in the network. We assume that at sink node k its random flow s_k has a mean e_k and variance σ_k^2 and that all the sinks are uncorrelated. Denoting $Q_{i,k}$ the flow through edge i in the single-sink state, i.e., only the kth sink is open with $s_k = 1$, we can obtain the decomposition $\langle Q_i^2\rangle = \sum_k \sigma_k^2 Q_{i,k}^2 + (\sum_k e_k Q_{i,k})^2$, which gives the averaged driving stimulus. In particular, if all the sinks are identically distributed, $e_k = e$ and $\sigma_k = \sigma$ $(k = 2, 3, \ldots, N)$, we have $\langle Q_i^2\rangle = \sigma^2 \sum_k Q_{i,k}^2 + e^2 \bar{Q}_i^2$, where $\bar{Q}_i$ is the flow through edge i in the all-sink state in which all the sinks are open with a unit flow rate s_k. It is interesting to observe that the averaged stimulus can be decomposed as a linear combination of the stimulus for all single-sink states $Q_{i,k}^2$ and the all-sink state $\bar{Q}_i^2$. By dimensional argument, it can be seen that different unit of the sink strength only leads to a change in the unit of conductivity. The topological structure of the network depends only on the ratio σ/e. This observation allows us to study optimal networks of sinks with this general randomness using the following model: We introduce a uniform open probability p and a uniform strength $1/\sqrt{p}$ for all sinks and select them to be open independently at each time according to the open probability. This network can be used to study the class of networks with random sinks which satisfies $\sigma/e = \sqrt{1-p/p}$, and the averaged stimulus satisfies

$$\langle Q_i^2\rangle = (1-p)\sum_k Q_{i,k}^2 + p\bar{Q}_i^2. \tag{3}$$

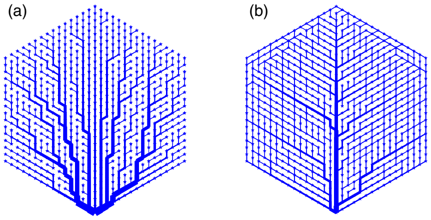

FIG. 1 (color online). Optimal structures for fixed sinks and fluctuating sinks. The width of an edge is proportional to $\tilde{C}^{1/3}$. The node at the bottom is the source point and the other nodes are all sinks. All edges between neighboring grids are possible edges of the network. In both cases, $\gamma = 0.5$. The initial conductivities are given as $1 + d$, where the perturbation d is uniformly distributed in the interval $[-0.5, 0.5]$. (a) Optimal structure obtained for fixed sinks, which is a loopless tree. (b) Optimal structure obtained with open-close-switching sinks ($p = 0.025$), which is covered by loops.

The all-sink case is obtained when $p = 1$, and the single-moving-sink case is obtained as $p \to 0$.

Simulation of adaptation dynamics.—The optimal structures are obtained from steady states of the adaptation dynamics (1) or (2) in our simulations [19].

Now we address the important question of how the open probability controls the optimal structures of the network. First, for the all-sink state, the optimal network has a treelike structure [Fig. 1(a)] for $\gamma < 1$ and a uniform sheet for $\gamma > 1$, with a phase transition at $\gamma = 1$. For $\gamma < 1$, there is a great number of locally optimal structures which can be obtained from different initial structures. This result is similar to those reported in Ref. [6] and can be similarly proven despite the different energy function used. Second, treelike structures can be obtained not only for the all-sink case but also for a large open probability. This can be seen in Fig. 2(a), which displays the relation between the loop density d_l and the open probability for different γ. As is shown in Fig. 2(a), the loop density is on average a decreasing function of p for fixed γ. Third, Fig. 2(a) suggests a high order phase transition in the network structures because of the existence of a critical open probability p_c [also shown in Fig. 2(b)], above which the optimal structure is loopless for $\gamma < 1$. Below p_c, the network exhibits hierarchical structures with loops. Figure 1(b) shows one such case, which resembles a leaf venation, full of small loops covering the

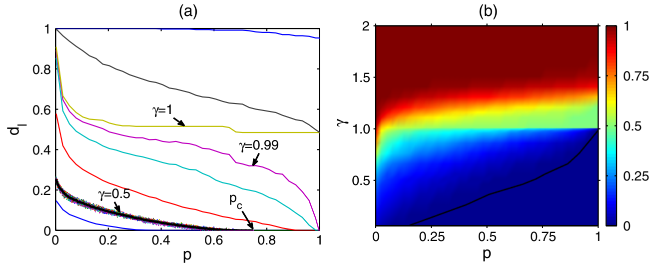

FIG. 2 (color online). The d_l-p curves for different γ (a) and the phase diagram for the loop density in the p-γ space (b). (a) Averaged loop densities are shown in solid lines from bottom left to top right for $\gamma = 0.25$, 0.5, 0.75, 0.95, 0.99, 1.0, 1.2, and 1.5. In addition, for $\gamma = 0.5$, there are 26 different realizations shown in colored dots to show the sensitivity of the loop number to realizations. (b) The critical point p_c obtained with our numerical simulations is shown by the solid curve. Below the curve, networks are loopless trees. The data are obtained from a network with 397 nodes and 1122 edges. The initial condition of conductivities is the same as that in Fig. 1.

entire network while maintaining an impression of treelike major veins [20]. The critical open probability p_c appears to be an increasing function of γ and it is also a slowly increasing function of the size of the network with an asymptotic limit as the network becomes large. The slope of d_l-p curves near the critical points becomes larger and larger as $\gamma \longrightarrow 1^-$. The d_l-p curves also suggest a nonuniform convergence of d_l as $\gamma \longrightarrow 1^-$ [21]. Fourth, for the all-sink case ($p = 1$), there is a phase transition at $\gamma = 1$. Figure 2(b) shows that, for sufficiently large p, there is also a rapid change in d_l across $\gamma = 1$, whereas for very small p, the change is smooth. Finally, we point out an intuitive understanding of why d_l decreases as p increases. Note that, as p increases, the second term on the right-hand side of Eq. (3) dominates. As a consequence, as $p \longrightarrow 1$, the behavior of optimal networks approaches that of the all-sink case, which possesses only a tree structure.

In summary, we have presented a model to describe the adaptation process of general biological transport networks in the presence of fluctuations in sinks (sources). Under this adaptation dynamics, the energy consumption of networks decreases and optimal structures are obtained as the steady states of the adaptation. In other words, in order to optimize the energy consumption, it is possible for a biological system to evolve to an adaptation process which responds only to local stimulus. In particular, loops are found in optimal networks when there are sufficient strong fluctuations in flow distribution. Comparing to the previous models on the adaptation of blood vessels [12,13], we have taken into account the effect of the open-close switch of capillary flow [14]. Our results may suggest a possible origin of the adaptation stability of anastomosis, which has been observed experimentally in arterial systems to form loops in arterial networks [12,13]. In contrast to the previous adaptation model on the network formed by *Physarum polycephalum* [16], our adaptation dynamics has a natural energy dissipation relation.

Our work provides a relation between the open probability of sinks and the loop density of a network and reveals a possible high order phase transition at the critical open probability. Note that it is possible to measure the open probability and area- or volumetric-loop density of a biological transport network in experiment. In addition, the power γ can be obtained by experimentally studying the scaling relation of the conductivities (diameters) of parent edges and their daughter edges in the network [7,18,22]. For example, Murray's law [18] provides a cubic relation between the diameter of a parent blood vessel and its two daughter vessels, and from this one can infer $\gamma = 1/2$ for blood vessel systems. Therefore, if one can relate the loop density defined in this work to the area- or volumetric-loop density, our relation between the loop density and the open probability may help us to examine the validity of our adaptation model and optimization principle for biological transport networks.

The work was supported by NSFC Grants No. 11004131, No. 91230202, and No. 11071161, NSF Grant No. DMS-1009575, and the NYU Abu Dhabi Institute under Grant No. G1301.

---

[*] hudan80@sjtu.edu.cn
[†] cai@cims.nyu.edu

[1] T. Nelson and N. Dengler, Plant Cell **9**, 1121 (1997).
[2] M. F. Laguna, S. Bohn, and E. A. Jagla, PLoS Comput. Biol. **4**, e1000055 (2008).
[3] E. Katifori, G. J. Szollosi, and M. O. Magnasco, Phys. Rev. Lett. **104**, 048704 (2010).
[4] F. Corson, Phys. Rev. Lett. **104**, 048703 (2010).
[5] S. Bohn and M. O. Magnasco, Phys. Rev. Lett. **98**, 088702 (2007).
[6] J. R. Banavar, F. Colaiori, A. Flammini, A. Maritan, and A. Rinaldo, Phys. Rev. Lett. **84**, 4745 (2000); M. Durand, *ibid.* **98**, 088701 (2007).
[7] M. Durand, Phys. Rev. E **73**, 016116 (2006).
[8] Borrowing the usage of Refs. [3,5], a uniform sheet is referred to as a network state in which there is no concentration tendency of conductances and the network is tiled with loops of uniform size.
[9] P. Dimitrov and S. W. Zucker, Proc. Natl. Acad. Sci. U.S.A. **103**, 9363 (2006).
[10] U. Pohl, J. Holtz, R. Busse, and E. Bassenge, Hypertension (Dallas) (1979-)/Hypertension **8**, 37 (1986); L. Kuo, W. M. Chilian, and M. J. Davis, Am. Physiol. Soc. **261**, H1706 (1991); A. Koller and G. Kaley, Am. J. Physiol. **260**, H862 (1991).
[11] W. J. G. Hacking, E. Vanbavel, and J. A. E. Spaan, Am. J. Physiol. Heart **270**, H364 (1996).
[12] A. R. Pries, T. W. Secomb, and P. Gaehtgens, Am. J. Physiol. Heart Circ. Physiol. **275**, H349 (1998); A. R. Pries, B. Reglin, and T. W. Secomb, Hypertension (Dallas) (1979-)/Hypertension **38**, 1476 (2001).

[13] Q. Chen, L. Jiang, C. Li, D. Hu, J. Bu, D. Cai, and J. Du, PLoS Biol. **10**, e1001374 (2012).

[14] D. Hu, D. Cai, and A. V. Rangan, PLoS One **7**, e45444 (2012).

[15] A. Kamiya, R. Bukhari, and T. Togawa, Bull. Math. Biol. **46**, 127 (1984).

[16] A. Tero, S. Takagi, T. Saigusa, K. Ito, D. P. Bebber, M. D. Fricker, K. Yumiki, R. Kobayashi, and T. Nakagaki, Science **327**, 439 (2010).

[17] J. B. Delashaw and B. R. Duling, Microvasc. Res. **36**, 162 (1988).

[18] C. D. Murray, Proc. Natl. Acad. Sci. USA. **12**, 207 (1926).

[19] In our simulation, the fourth order Runge-Kutta method is used to solve the adaptation dynamics until the steady state is reached. In the adaptation dynamics (1), Kirchoff's law is directly used to determine the pressure and flow rate of the all-sink state at each time step. In the adaptation dynamics (2), the pressures and flow rates of all single-sink states are obtained simultaneously by finding the inverse matrix in Kirchoff's law for the pressures. The flow rate of the all-sink state is obtained by the sum of all the single-sink states and Eq. (3) is used to obtain the averaged stimulus in the adaptation dynamics (2). In this approach, for any given open probability p, the computational cost of each step is almost the same as that for the case of single-moving sink [3].

[20] From Eq. (2), we have $\langle Q_i^2 \rangle = \tilde{\tau}_e^2 \tilde{C}_i^{\gamma+1}$ at steady states. Therefore, we can obtain the averaged flow rate in an edge by its conductivity. For treelike optimal structures, the flows can only take the discrete values, $\langle Q_i^2 \rangle = n_i(e^2 + \sigma^2)$, where n_i is the number of downstream nodes of edge i, and the end branches have the value of the low bound of averaged flow, $\sqrt{e^2 + \sigma^2}$. However, for optimal structures with loops, the flow is continuously distributed and has no lower bound.

[21] This nonuniform convergence of the loop density as $\gamma \rightarrow 1$ is signified in Fig. 2(a) by a sudden jump of d_l from $\gamma \rightarrow 1$ to $\gamma = 1$ at $p = 1$.

[22] C. A. Price, S. Wing, and J. S. Weitz, Ecol. Lett. **15**, 87 (2012).